Astrophys Space Sci (2019) 364:71
https://doi.org/10.1007/s10509-019-3562-8

ORIGINAL ARTICLE

The high energy emission of the Crab's twin pulsar PSR J0540-6919 in the Large Magellanic Cloud

G. Machabeli[1] · A. Rogava[1] · N. Chkhidze[1] · N. Kevlishvili[1]

Received: 23 November 2018 / Accepted: 16 April 2019 / Published online: 24 April 2019

Abstract In the present paper, we discuss theoretical interpretation of the X-ray and gamma-ray emission of the extremely bright pulsar PSR J0540-6919, in the Large Magellanic cloud. The source of the high frequency emission is assumed to be the synchrotron radiation, which is generated near the light cylinder during the quasi-linear stage of the cyclotron instability developed in this region. The emitting particles are the particles of the primary beam, with the Lorentz factors of the order of $\gamma_b \sim 10^7$ that provide generation of the gamma-ray emission with the photon energy up to 10 GeV and the secondary plasma electrons with $\gamma_t \sim 10^5$, emitting in the X-ray domain. The theoretical synchrotron radiation spectra obtained in the framework of the model provide natural explanation of the observed photon spectra showing power-law indices 2.2 for gamma-rays and 1.55 for the X-rays. The present model provides natural explanation for pulse-aligned emission peaks at different frequencies and smearing of two-peak pulse profile at higher frequencies that is clearly observed in radio domain.

Keywords Pulsars · Individual: PSR J0540-6919 · Radiation mechanisms: non-thermal

1 Introduction

Recently the Fermi-LAT collaboration reported detection of pulsed GeV gamma-rays from the young pulsar PSR J0540-6919 (hereafter J0540) in the Large Magellanic Cloud (Ackermann et al. 2015), which is the first gamma-ray pulsar detected in another galaxy. Although, J0540 shares many similarities with the Crab pulsar and is often called "Crab's twin", its isotropic, pulsed gamma-ray emission exceeds the Crab pulsar's by a factor of 20. The spin period of this pulsar is $P = 50$ ms, the rotation power is $\dot{E} = 1.5 \times 10^{38}$ erg s^{-1}, while the magnetic field strength at the light cylinder is $B_{LC} = 3.62 \times 10^5$ G. Similarly to the Crab pulsar, J0540 reveals the pulsed emission in radio, X-ray and optical domains, and it is very important to note that these emission components are aligned. However, unlike the case of the Crab pulsar which shows a sharp double-peak structure, the shape of the pulse for J0540 varies over the different bands (see Fig. 2 in Ackermann et al. 2015). In particular, the pulsed radio emission exhibits two narrow peaks separated by $\Delta \sim P/4$ in pulse phase and for the higher frequencies the double-peak pattern is not that clearly pronounced, but it can be still noticed on the top of a broader profile (like a dip). However, the phase-alignment of the measured signal peaks seems to indicate that the emission in different energy bands is generated in the same spatial region of the pulsar magnetosphere. Moreover, similarly as the Crab pulsar J0540 emits the giant radio pulses that appear at the positions of the pulse peaks in higher-energy bands (Johnston et al. 2004).

In the present paper we develop a model that explains the presence of the phase-alignment of these signals. The model naturally leads to the explanation of other observed emission features of the J0540 pulsar. We assume that the observed emission is formed in the electron-positron ($e^- e^+$) plasma of the pulsar magnetosphere. The basis for the pulsar emission models is the process of the birth of electron-positron pairs (Klepikov 1954; Deutsch 1955; Erber 1966; Goldreich and Julian 1969; Sturrock 1971; Ruderman and Sutherland 1975; Michel 1982). A spinning magnetized neutron star generates an electric field directed along the open magnetic field lines that extracts electrons from the star's surface

✉ G. Machabeli
g.machabeli@iliauni.edu.ge

[1] Centre for Theoretical Astrophysics, ITP, Ilia State University, G. Tsereteli 3, Tbilisi 0162, Georgia

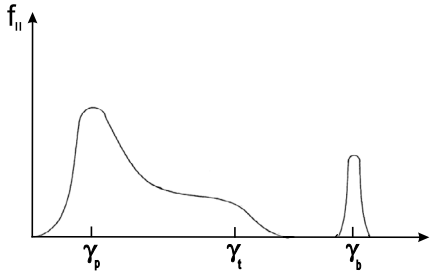

Fig. 1 Distribution function for a one-dimensional electron-positron plasma of pulsar magnetosphere

forming a low number density ($n_{b_0} = B_0/(ceP)$ plasma, where B_0 is the magnetic field at the star's surface, P is the pulsar spin period, e is the electron's charge and c is the speed of light) primary beam of particles with energies $\gamma_b \sim 10^6$–10^7 (Goldreich and Julian 1969). The beam particles moving along the magnetic field lines radiate γ-quanta, which, in turn, produce electron-positron pairs. The pitch angle of the particles which are being produced is non-zero, so that secondary particles generate synchrotron radiation. This radiation, in turn, produces more and more pairs until the plasma becomes sufficiently dense to screen the 'parent' electric field. As a result a multicomponent magnetospheric plasma is formed. In this medium different plasma processes may develop, resulting in emission generation, observed as a pulsed radiation from pulsars.

The paper is organized as follows. In Sect. 2 we describe the emission model, in the Sect. 3, on the basis of our model, we derive the theoretical synchrotron spectrum for the X-day and the very high energy γ-ray emission of the J0540 pulsar, in Sect. 4 we make the interpretation of observed hight energy spectra in the framework of present model and in the Sect. 5 we make conclusions.

2 Emission model

Generally pulsar emission models suggest that the multi-wavelength pulsed radiation is generated in the magnetospheric e^-e^+ plasma, which has a one-dimensional distribution (Fig. 1 Tademaru 1973; Arons 1981). This is due to lost of any transverse momenta in a very short time via synchrotron emission in very strong surface magnetic fields. The distribution function consists of the following two components:

- the bulk of plasma with the particle concentration at the neutron star's surface $n_p \approx 10^{18\text{–}19}$ cm^{-3} and the Lorentz-factor $\gamma_p \approx 10^2$ (in case of dipolar magnetic field) or $\gamma_p \approx$ (3–10) (in case of quadrupole magnetic field) (Machabeli and Usov 1989);
- the long, extended, one-dimensional tail of the distribution function with $\gamma_t \approx (10^3$–$10^5)$, $n_t \approx (10^{16}$–$10^{17})$ cm^{-3}

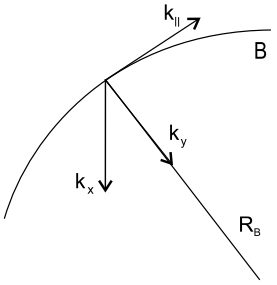

Fig. 2 The coordinate system with the parallel component of the wave vector directed tangentially to the local magnetic field

- and the most energetic primary beam with $\gamma_b \approx (10^6$–$10^7)$ and $n_b \approx 10^{13}$ cm^{-3} (Goldreich and Julian 1969).

The one-dimensionality of the distribution function is a reason for the development of the plasma instabilities that results in generation of e^-e^+ eigen-waves. Another factor is the form of the distribution function of the plasma particles. For the magnetospheric e^-e^+ plasma the distribution function $f_0(\gamma)$ contains areas, where $\partial f_0/\partial\gamma > 0$ and the anisotropic form ensures unstableness of such plasma and excitation of waves.

One of the essential plasma processes that makes the one-dimensional plasma unstable is cyclotron-Cherenkov instability, developing at the anomalous cyclotron resonance (Lominadze et al. 1979; Machabeli and Usov 1979b; Lominadze et al. 1983; Kazbegi et al. 1991; Lyutikov et al. 1999)

$$\omega - k_\parallel \upsilon_\parallel - k_x u_x = -\frac{\omega_B}{\gamma_r}, \tag{1}$$

here γ_r is the Lorentz factor of the resonant particles, $u_x = c\upsilon_\parallel\gamma_r/\omega_B R_B$ is the drift velocity of the particles, $\omega_B = eB/mc$ is the cyclotron frequency, R_B is the curvature radius of the magnetic field lines and the resonance condition is written for the weakly inhomogeneous magnetic field case. The weak inhomogeneity results in a curvature drift motion of the particle perpendicular to the local plane of the magnetic field line (see Fig. 2).

In vacuum conditions the anomalous Doppler effect can not be realized. As the estimations show, for the typical pulsar parameters, wave excited through the anomalous cyclotron resonance belong to the radio frequency range. At the quasilinear stage of this process the generated radio waves affect inversely the unperturbed distribution function and lead to the particle diffusion along and across the magnetic field. This, in its turn, leads to the stabilization of the instability. Through this process the particles obtain the perpendicular momenta and start to radiate via the synchrotron mechanism in much higher frequency domains. Therefore, the radio and high frequency emission are both generated simultaneously and in the same spatial location of the pulsar magnetosphere that may naturally explain the observational evidence for the pulse-peak coincidence for different frequency ranges. In the present work we investigate in more details the anomalous cyclotron resonance and apply it for

the explanation of the observed emission properties of the J0540 pulsar.

In order to analyze the resonance condition (1), one needs to know the properties of the fundamental modes of e^-e^+ plasma. They were investigated in a series of works Volokitin et al. (1985), Arons and Barnard (1986), Kazbegi et al. (1991), Lyutikov et al. (1999). It was shown that in e^-e^+ three branches of wave modes can propagate tangentially to the magnetic field lines: the purely transversal mode with electric field perpendicular to **k**–**B** plane and longitudinal-transverse waves with the electric field in the **k**–**B** plane with two branches: the ordinary and the Alfvén mode. For small angles of propagation with respect to the magnetic field ($k_\perp/k_\parallel \ll 1$) the dispersion relations for these waves in the laboratory frame can be written as:

$$\omega^t = kc(1-\delta), \tag{2}$$

$$\omega^{lt} = k_\parallel c\left(1-\delta-k_\perp^2 c^2/4\gamma_p\omega_p^2\right), \tag{3}$$

$$\left(\omega^{Lt}\right)^2 = \omega_p^2\gamma_p^{-3} + k_\parallel^2 c^2. \tag{4}$$

Here $\delta = \omega_p^2/4\gamma_p^3\omega_B^2$, $\omega_p^2 = 4\pi^2 n_p/m$. It should be noted that these waves are frequently called X, O and A modes. We consider in detail the excitation of an extraordinary (X) mode, hereafter referred to as "t-waves".

Let us insert the expression (2) into resonance condition (1) and use the expansions for the following quantities $\upsilon_\parallel \approx c(1-1/2\gamma_r^2 - u_x^2/2c^2)$, $k = k_\parallel(1+k_\perp^2/k_\parallel^2)^{1/2} \approx k_\parallel(1+k_\perp^2/2k_\parallel^2)$ and $k_\perp = (k_x^2+k_y^2)^{1/2}$, then we will get

$$\frac{1}{2\gamma_r^2} + \frac{1}{2}\left(\theta - \frac{u_x}{c}\right)^2 + \frac{k_y^2}{2k_\parallel^2} - \delta \approx -\frac{\omega_B}{\gamma_r k_\parallel c}. \tag{5}$$

The first three terms on the left hand-side of the Eq. (5) are positive and it is clear that in order to satisfy this equation one needs the following condition to be satisfied:

$$|\delta| > \frac{1}{2\gamma_r^2} + \frac{1}{2}\left(\theta - \frac{u_x}{c}\right)^2 + \frac{k_y^2}{2k_\parallel^2}. \tag{6}$$

However, this condition does not exclude the possibility of the equality $\theta \approx u_x/c$, which guarantees that the condition (6) holds for the resonant particles with the high Lorentz factors. The mentioned condition, when $k_y^2 \sim k_x^2$ will take the form:

$$|\delta| > u_x^2/2c^2. \tag{7}$$

When the following condition is satisfied:

$$\theta \approx u_x/c, \tag{8}$$

the emission beams coming from radiation generation region form tapered segment and the section of this cone has the shape shown on Fig. 3. If the observer's line of sight intersects the hollow part of the cone then the detected emission will have the observed two-peak profile. This type of emission is frequently called 'conal-emission' (Rankin 1983). The angular distance between the pulse peaks is defined from the condition (8). Although, it should be mentioned that the presence of two-peaks in the emission profile can be also interpreted in other ways: the orthogonal rotator or the almost aligned rotator (Manchester and Taylor 1977). However, for the first case the distance between the peaks must be of the order of 180° and for the second case generation of the emission from different frequency bands happens in different locations in the pulsar magnetosphere and it is not possible to have the pulse-phase coincidence for them.

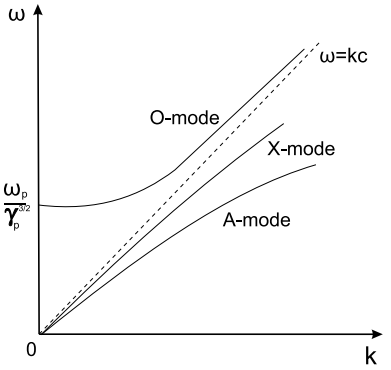

Fig. 3 Dispersion curves for the eigen-waves in a magnetized electron-positron plasma for oblique propagation (Machabeli et al. 1999)

Let us estimate the quantities θ and δ. Assuming that at the star surface $n_p \sim 10^{19}$ cm^{-3} and that this quantity reduces with a cubic law, just like the magnetic field does, the number density of the plasma particles at the light cylinder distances will be $n_p^{LC} \sim n_p(r_0/r_{LC})^3$ (where $r_0 \approx 10^6$ cm is the neutron star radius and $r_{LC} \sim 10^8$ cm is the radius of the light cylinder—the distance from the pulsar, where the linear velocity of rotation matches the speed of light). According to Ackermann et al. (2015) one can write for the magnetic field at the light cylinder $B_{LC} \approx 3.6 \times 10^5$ G. Consequently we will get $\delta \approx 7 \times 10^{-6}$.

From the resonance condition (5) one can estimate the frequency of the waves generated through the cyclotron resonance:

$$\nu_c = \omega_c/2\pi \approx k_\parallel c = \omega_B/\gamma_r\delta. \tag{9}$$

The region where the waves are generated is located in the periphery area of the magnetosphere near the light cylinder zone. In reality, when the light cylinder surface is being approached, the magnetic field lines start to bend in the opposite direction of the star rotation. Consequently, this is the area where the magnetic field lines start to change their actual curvature (let us assume that $R_B \sim 10^7$ cm). From the expression (9) one can see that near the light cylinder radio

waves of the order of 1 GHz are generated when the resonant particles are the fastest primary beam electrons with the Lorentz factors $\gamma_r \sim 10^7$. In this case $\theta \approx u_x/c \approx 0.01$, which comes in agreement with the estimated distance between the pulse peaks from the observations (Ackermann et al. 2015).

Frequently from pulsar observations modes with the orthogonal electric fields (Manchester and Taylor 1977) are found. This observable feature is very natural for the plasma model presented in this work, as in pulsar pair plasma both t and lt waves are generated. Now let us consider excitation of lt waves through the cyclotron resonance. The dispersion relation for these waves is described by Eq. (3) and after applying it to the resonance condition (1) one can get:

$$\left(\delta + \frac{k_\perp^2 c^2}{4\gamma_p \omega_p^2} + \frac{k_x^2}{2k_\parallel^2}\right) - \frac{1}{2}\left(\frac{k_x}{k_\parallel} - \frac{u_x}{c}\right)^2 = \frac{\omega_B}{\gamma_r k_\parallel c}. \tag{10}$$

From this equation one can see that the second term has no impact on the wave generation condition, which implies that the lt-waves fill the entire emission cone when generated through the anomalous Doppler resonance. The wave generation takes place in a small angle range, for lt waves $\theta \ll 1$. Contrary to this, for the t-waves, the emission beams are limited from both sides $u_x^2/c^2 = \theta^2 < 2\delta$ (see condition (7)). It is worthwhile to note that, while generated via the Cherenkov resonance, both t and lt waves are forming the hollow cone (Kazbegi et al. 1991; Lyutikov et al. 1999a). We assume that the absence of the second mode and the high linear polarization of the radio pulses at 1 GHz would be a good argument in favour of our emission model.

3 Quasi-linear diffusion and the high frequency synchrotron spectra

In this section we consider processes taking place in e^-e^+ plasma in the area, which is much smaller than value of R_B. The pair plasma in the pulsar magnetosphere bears cylindrical symmetry and it is convenient to describe the processes in the momentum space in the cylindrical coordinates. After the average over the azimuthal angle is found, the process can be described in two-dimensional space of momenta $p_\parallel$ and $p_\perp$ along and across the magnetic field lines. The back reaction of the generated waves on the resonant particles' distribution function in the e^-e^+ plasma is described via the quasi-linear equation (Lominadze et al. 1979; Machabeli and Usov 1979a; Melrose 1980; Lominadze et al. 1983; Kazbegi et al. 1992). We are interested to find the function $f_\perp$, which describes the particle distribution across the magnetic field after the quasi-linear diffusion causes the particle redistribution. The equation describing this process can be written as (Chkheidze et al. 2013):

$$\frac{\partial f_\perp}{\partial t} = \frac{1}{p_\perp}\frac{\partial}{\partial p_\perp}\left[p_\perp D_{\perp,\perp}\frac{\partial f}{\partial p_\perp} - p_\perp F_\perp f\right]. \tag{11}$$

Here the perpendicular component of the synchrotron radiation reaction force is:

$$F_\perp = \alpha_s \frac{p_\perp}{p_\parallel}\left(1 + \frac{p_\perp^2}{m^2c^2}\right), \quad \alpha_s = -\frac{2e^2\omega_B^2}{3c^2}. \tag{12}$$

and the diffusion coefficient:

$$D_{\perp,\perp} = \frac{e^2}{8c}\delta|E_k|^2_{k=k_{res}}. \tag{13}$$

The term containing the orthogonal diffusion coefficient in Eq. (11) ensures appearance of perpendicular momenta and their growth and the term containing the orthogonal reaction force slows this process down. It leads to the balance of the processes and the perpendicular distribution function will remain stationary $\partial f_\perp/\partial t = 0$. The Eq. (11) in this case has a simple solution. When the condition $\gamma_r\psi \ll 1$ is met one can write it as:

$$f_\perp \propto e^{-(\frac{\psi}{\psi_0})^2}, \tag{14}$$

here $\psi \approx (p_\perp/p_\parallel) \ll 1$ is the pitch angle of the resonant particles and the mean value of the pitch angle has the following, different value:

$$\psi_0 = \frac{p_{0\perp}}{p_\parallel} = \frac{1}{\omega_B^2}\left(\frac{3c\omega_p^2}{32p_\parallel\gamma_p^3}|E_k|^2\right)^{1/2}. \tag{15}$$

The process of quasi-linear diffusion causes appearance of pitch angles that inevitably causes activation of the synchrotron radiation mechanism. As the resonant particles are the fastest beam electrons, they emit a high-frequency radiation through the synchrotron regime. Indeed, the characteristic photon energy emitted by relativistic electrons through the synchrotron radiation process is $\epsilon_{syn} \approx 5 \times 10^{-18} B\psi\gamma^2$ GeV (Ginzburg 1981). If we use Eq. (15) for the mean value of the pitch angle (assuming that the conditions $\gamma_r\psi \ll 1$ is satisfied for this pulsar), where one can assume $|E_k|^2 \approx mc^3 n_b\gamma_b/(2\omega_c)$, we obtain (Chkheidze et al. 2013)

$$\epsilon_{syn}(\mathrm{GeV}) \simeq 5 \times 10^{-18}\frac{\pi}{\gamma_p^4 B}\left(\frac{3m^5c^7\gamma_b^7}{16e^6P^3}\right)^{1/2}. \tag{16}$$

The estimations show that the beam electrons with the Lorentz factor $\gamma_b \sim 10^7$ radiate γ-photons with the energy of the order of 10 GeV. Consequently, the optical and X-ray emission is generated via secondary plasma electrons $\gamma_p \sim 10^3$ and $\gamma_t \sim 10^5$. These secondary plasma particles

generate through the described mechanisms the radio emission at different frequencies. Consequently, for different radio frequencies the angle $\theta \approx (u_x/c)$ should differ. This interesting circumstance can be used to test the present model.

The synchrotron emission has the different nature from radio emission and the conditions (7) and (8) do not play a role for it. Unlike the radio emission case, the wavelength of the high-frequency emission is $\lambda \ll n_p^{-1/3}$. Therefore, the waves do not feel the medium and there is no need to take into account the wave interference. We assume that the broadening of the pulse profile in the higher frequency range can be explained via redistribution of particles by pitch angles. It is worth noting that flattening of pulse profiles for the optical, X-ray and gamma-ray emission is also observed for the Crab pulsar (Manchester and Taylor 1977). It is clear that when the above described processes develop the resultant synchrotron emission power is fed by the longitudinal kinetic energy of the resonant particles, which is also partly spent on the radio wave generation. The maximum intensity of the high-frequency emission comes on the maximum photon quantity, while the latter is proportional to the density of emitting particles multiplied on their Lorentz factor.

The spectral density of synchrotron emission photon flux of the bunch of particles can be written as (Chkheidze et al. 2013)

$$F_\epsilon \propto \int_{p_{\parallel min}}^{p_{\parallel max}} f_\parallel(p_\parallel) B \psi_0 \frac{\epsilon}{\epsilon_{syn}} \left[\int_{\epsilon/\epsilon_{syn}}^{\infty} K_{5/3}(\chi) d\chi \right] dp_\parallel, \tag{17}$$

here $f_\parallel$ is the longitudinal distribution function of the emitting particles and can be found from the following equation (Chkheidze et al. 2013)

$$\frac{\partial f_\parallel}{\partial t} = \frac{\partial}{\partial p_\parallel} \left[\frac{\alpha_s}{m^2 c^2} \frac{1}{\omega_B^4} \frac{3 c \omega_p^2}{32 \gamma_p^3} p_\parallel |E_k|^2 f_\parallel \right]. \tag{18}$$

Considering the quasi-stationary state we find

$$f_\parallel \propto \frac{1}{p_\parallel |E_k|^2}. \tag{19}$$

For the density of the electric energy in the excited waves one can write

$$\frac{\partial |E_k|^2}{\partial t} = 2 \Gamma_c |E_k|^2, \tag{20}$$

where $\Gamma_c = \pi^2 e^2 f_\parallel / k_\parallel$ is the growth rate of the instability.

From Eqs. (18) and (20) one can find

$$|E_k|^2 \propto p_\parallel^{-n+1}, \tag{21}$$

where it has been taken into account the following assumption for the initial distribution function of the resonant particles $f_{\parallel_0} \propto p_\parallel^{-n}$.

Using the expressions (19), (21) and (15) and replacing the integration variable $p_\parallel$ with $x = \epsilon/\epsilon_{syn}$ in the integral (17) one obtains

$$F_\epsilon \propto \epsilon^{-\frac{n-6}{n-4}} \int x^{\frac{n-6}{n-4}} \left[\int_x^\infty K_{5/3}(\chi) d\chi \right] dx. \tag{22}$$

The integral (22) can be approximately expressed with the following equation:

$$F_\epsilon \propto \epsilon^{-\frac{n-6}{n-4}} \exp\left[-\frac{\epsilon}{\epsilon_0} \right], \tag{23}$$

here ϵ_0 corresponds to cutoff energy of the power-law synchrotron spectrum and can be numerically calculated for different energy intervals for the integration.

For effectiveness of the current emission model it is essential that the time of wave-particle quasi-linear interaction is more than the growth time of the cyclotron-Cherenkov instability $(1/\Gamma_c)$. Generated radio waves propagate practically in straight lines, whereas the field line of the dipole magnetic field deviates from its initial direction, and the angle θ grows. The resonance condition (1) limits the angle θ for which the particles can resonate with the generated waves. Consequently, the wave-particle interaction sustains until the following condition is fulfilled (Kazbegi et al. 1991; Lyutikov et al. 1999)

$$R_B \theta \gtrsim \frac{c}{\Gamma_c}, \quad \Gamma_c = \frac{\pi \omega_b^2 u_x^2}{2 \omega_c \delta c^2 \gamma_T}, \text{ if } \delta \ll \frac{1}{2} \frac{u_x^2}{c^2}. \tag{24}$$

Here $R_B \theta$ is the length of wave-particle interaction, $c^{-1}\Gamma_c$ is the growth length, $\omega_b^2 = 4\pi^2 n_b/m$ and γ_T is the half-width of the distribution function of resonant beam particles (according to the fit results $\gamma_T \sim 10^7$, see below). As the estimations show, this condition is well fulfilled in the vicinity of the light cylinder zone and there is enough time for the instability to develop.

4 Theoretical interpretation of X-ray to Gamma-ray spectra

In the X-ray domain J0540 was observed with different satellites and its X-ray spectrum is described by various authors as a power law with photon indices in the range from 1.8 to 2.0 de Plaa et al. (2003), Campana et al. (2008). For analyzing the X-ray emission of this pulsar we refer to data collected by two satellites, the Swift and the RXTE that observed J0540 several times. In particular, XRT instrument on board of Swift satellite was used for the observations that provided data in 0.7–7.14 keV energy interval. In case of RXTE satellite two different instruments were used for the observations, PCA that provided data in the 2–30 keV energy interval and HEXTE providing data in the 15–250 keV

energy interval. All three spectra were fitted individually and then simultaneously with XSPEC v. 12.8.2 and to account the interstellar absorption we have referred to *wabs* in XSPEC. Using the command *mdefine*, we defined the model for fitting according to our theoretical spectrum (expression (23), were we denoted the index of the power law in the following way $(n-6)/(n-4)=\beta$). The resulting best-fit parameters are $\beta = 1.55 \pm 0.09$, $\epsilon_0 = 23.8 \pm 5.7$ keV and $N_H = (2.6 \pm 0.2) \times 10^{21}$ cm^{-2}, with $\chi^2 = 0.88$ for 136 degrees of freedom (see Fig. 4). This implies for the $n = 1.63$ in expression (23) that shows the initial distribution function of the tail of the secondary plasma electrons. As mentioned above the tail of the distribution function of secondary plasma is extended over the Lorentz factors $\gamma_t \simeq (10^3$–$10^5)$. For these values the integral (22) gives that the cutoff energy in expression (23) equals $\epsilon_0 \approx 20$ keV that comes in good agreement with the measured spectrum.

According to the observations the high energy gamma-ray spectrum is well described by power-law with the index 2.2 ± 0.1 and exponential cutoff at $E_{cutoff} = 7.5 \pm 2.6$ GeV (Ackermann et al. 2015). In order that the theoretical spectrum obtained in the framework of synchrotron emission model fits the observations, the value of the n should be equal to 2.3, which is a reasonable value for the index of the initial distribution function of the primary beam electrons that provide emission in the gamma-ray domain. In order to fit well the observed data we assume that energy of the beam electrons varies in the interval $\gamma_{min} \simeq 10^6$ and $\gamma_{max} \simeq 5 \times 10^7$, in which case from integral (22) we obtain that the value of the cutoff energy in the expression (23) equals $\epsilon_0 \approx 8$ GeV that comes in good agreement with the measured spectrum (see Fig. 5).

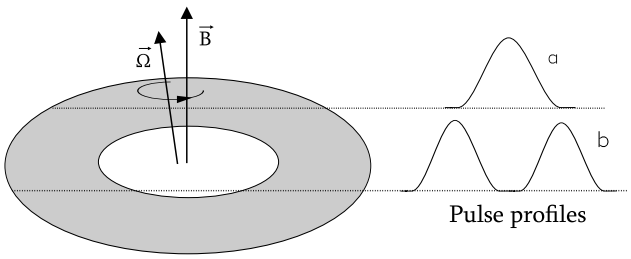

Fig. 4 The possible pulse-profile shapes for the radio emission of the pulsar generated via the anomalous Doppler resonance

5 Conclusions

In this paper some aspects of the extremely bright gamma-ray pulsar in the Large Magellanic Cloud (J0540) are considered. They are easily interpreted in the framework of the pulsar emission model developed in Lominadze et al. (1979), Machabeli and Usov (1979a), Lominadze et al. (1983), Kazbegi et al. (1991), Lyutikov et al. (1999). In particular we found out that:

1. The possibility of the instability development is considered, which leads to the generation of radio emission at the anomalous Doppler resonance.
2. It is demonstrated that at this resonance a "conal" type of emission can be generated. We argue that this could explain the presence of the double peak radio emission feature.
3. It is shown that at the quasilinear stage of the instability development the one-dimensional distribution function will acquire pitch angles. The latter provides the possibility for the generation of the high-frequency synchrotron emission.
4. The theoretical synchrotron spectra are calculated for the presented model that provides a good explanation of the measured X-ray and Gamma-ray spectra.

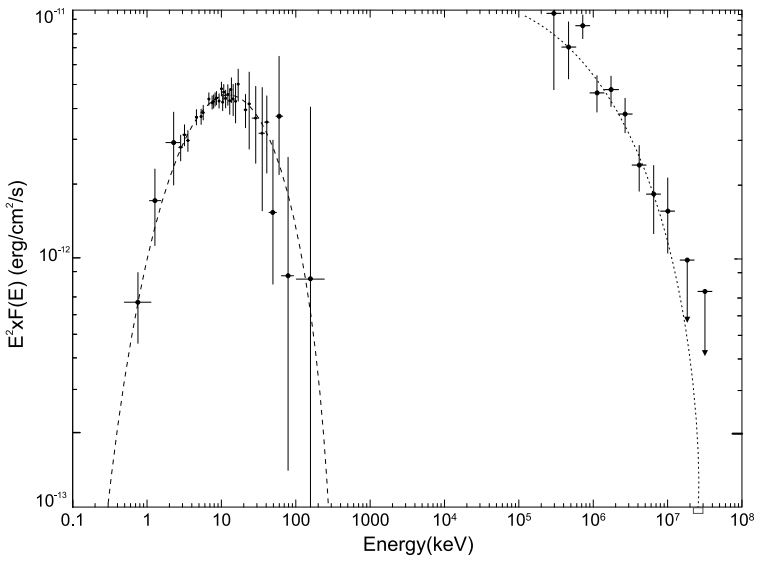

Fig. 5 The pulsed spectrum of PSR J0540-6919 from X-ray in the energy interval 0.7–250 keV (Swift/XRT and RXTE/PCA-HEXTE data) up to Gamma-rays of the energy of 10^{10} GeV

5. Simultaneous generation of radio and high-frequency emission in the same, spatially confined domain naturally explains the observed coincidence of the emission peaks at different frequencies (phase-alignment).
6. Numerical studies show good agreement of the theoretical estimation of the distance between the peaks in radio range with the observed one.
7. In the framework of the suggested model, on the basis of the quasilinear diffusion calculation, the distribution over the pitch angles is determined. The latter naturally explains the observed broadening of the pulses at higher frequencies relative to radio pulse shapes.
8. Often in pulsar emission subpulses two different modes are detected with mutually orthogonal electric fields (Manchester and Taylor 1977), which is quite expectable because both t and lt waves are generated. In our case the presence of double peaks at the frequency of the order of GHz is interpreted as the "conal" emission generated at the anomalous Doppler resonance. We have shown that this kind of emission is possible only for t-waves. Therefore, observed radio emission pulses of the order GHz has to be characterized by the high degree of linear polarization and the absence of the second mode.
9. A generic connection between low-frequency (10^{13}–10^{18} Hz) and high-frequency (from the optical to X-rays and gamma-rays) emission is found. It turns out that Lorentz factors for the generation of optical and X-ray emission have to be 10^3 and 10^5, respectively. It has to lead to difference of the distance between the peaks in the radio range for different frequencies. It may be used as an important observational test for the verification of the suggested model.

Acknowledgements We are grateful to Dr. Riccardo Campana for helpful advices and providing the observational data. The work was supported by Shota Rustaveli National Science Foundation of Georgia (SRNSFG) [FR17_587].

References

Ackermann, M., et al. (Fermi LAT Collaboration): Sci. **350**, 801F (2015)
Arons, J.: In: Proc. Varenna Summer School and Workshop on Plasma Astrophysics, p. 273. ESA (1981)
Arons, J., Barnard, J.J.: Astrophys. J. **302**, 120 (1986)
Campana, R., Mineo, T., De Rosa, A., et al.: Mon. Not. R. Astron. Soc. **389**, 691 (2008)
Chkheidze, N., Machabeli, G., Osmanov, Z.: Astrophys. J. **773**, 143 (2013)
de Plaa, J., Kuiper, L., Hermsen, W.: Astron. Astrophys. **400**, 1013 (2003)
Deutsch, A.J.: The electromagnetic field of an idealized star in rigidrotation in vacuo. Rev. Mod. Phys. **38**, 626 (1955)
Erber, T.: High-energy electromagnetic conversion processes in intense magnetic fields. Rev. Mod. Phys. **38**, 626 (1966)
Ginzburg, V.L.: Teor. Fizika i Astrofizika. Nauka, Moscow (1981)
Goldreich, P., Julian, W.H.: Pulsar electrodynamics. Astrophys. J. **157**, 869 (1969)
Johnston, S., Romani Roger, W., Marshall, F.E., Zhang, W.: Mon. Not. R. Astron. Soc. **355**, 31J (2004)
Kazbegi, A., Machabeli, G., Melikidze, G.: Mon. Not. R. Astron. Soc. **253**, 377 (1991)
Kazbegi, A., Machabeli, G., Melikidze, G.: msem.coll. 232K (1992)
Klepikov, N.P.: Izluchenie fotonov v elektronno-pozitronnoi plazme. J. Exp. Theor. Phys. **26**, 19 (1954) (in Russian)
Lominadze, J.G., Machabeli, G.Z., Mikhailovskii, A.B.: Fiz. Plazmy **5**, 1337 (1979)
Lominadze, J.G., Machabeli, G.Z., Usov, V.V.: Astrophys. Space Sci. **90**, 19L (1983)
Lyutikov, M., Blandford, R.D., Machabeli, G.: Mon. Not. R. Astron. Soc. **305**, 338 (1999)
Lyutikov, M., Machabeli, G., Blandford, R.: Astrophys. J. **512**, 805 (1999a)
Machabeli, G.Z., Usov, V.V.: Sov. Astron. Lett. **5**, 238 (1979a)
Machabeli, G.Z., Usov, V.V.: Pis'ma Astron. Zh. **5**, 445 (1979b)
Machabeli, G.Z., Usov, V.V.: Cyclotron instability and the generation of radio emission in pulsar magnetospheres. Sov. Astron. Lett. **15**, 393 (1989)
Machabeli, G.Z., Vladimirov, S.V., Melrose, D.B.: Phys. Rev. E **59**, 4552 (1999)
Manchester, R.N., Taylor, J.H.: Pulsars. Freeman, San Francisco (1977)
Melrose, D.B.: Plasma Astrophysics: Nonthermal Processes in Diffuse Magnetized Plasmas. Gordon & Breach, New York (1980)
Michel, F.C.: Theory of pulsar magnetospheres. Rev. Mod. Phys. **54**, 1 (1982)
Rankin, J.M.: Astrophys. J. **274**, 333 (1983)
Ruderman, M.A., Sutherland, P.G.: Theory of pulsars—polar caps, sparks, and coherent microwave radiation. Astrophys. J. **196**, 51 (1975)
Sturrock, P.A.: A model of pulsars. Astrophys. J. **164**, 529 (1971)
Tademaru, E.: Astrophys. J. **183**, 625 (1973)
Volokitin, A.S., Krasnoselskikh, V.V., Machabeli, G.Z.: Fiz. Plazmy **11**, 531 (1985)